RSC Advances

ROYAL SOCIETY
OF CHEMISTRY

www.rsc.org/advances

RSC Advance

FULL PAPER

Unravelling the photo-excited chlorophyll-a assisted deoxygenation of graphene oxide: Formation of nanohybrid for oxygen reduction

Debmallya Das[a†], Jhimli sarkar Manna[b,c†]*, Manoj Kumar Mitra[a]

We tried to expand the horizon of graphene oxide (GO) reduction methods through chlorophyll-a (CHL-a) molecules which is inclined to react favourably with GO by virtue of photo excited electron transfer from singlet excited CHL-a LUMO [-0.7volt] to GO [-0.4] in aqueous media favoured by the interactive affinity between CHL-a and reduced graphene oxide (RGO), which is ensured through π-π interaction between CHL-a macro-cycle and GO surface, resulting in the formation of CHL-a$^+$ radical cation which might favor the oxidation of water with oxygen evolution. The formation of RGO after photo-exposure also can be confirmed via TEM and Raman spectra measurement. Gradual restoration of sp2 hybridisation in GO frame work with increasing CHL-a concentration can be correlated with the enhanced contribution of the conformation in which electron transfer is efficient from CHL-a to GO, [also supported by XPS and XRD data] this fact corroborates the faster component augmentation towards overall excited state life time. The applicability of this GO/CHL-a nano-hybrid as a possible electro-catalyst, to be used for oxygen reduction in energy conversion systems such as fuel cell has also been explored through cyclic voltammetry. All these results cumulatively highlight towards an effective environment friendly mechanism of the photo-excited CHL-a assisted deoxygenation of GO in aqueous media, which eventually give rise to RGO/CHL-a nano-hybrid as an potential electro-catalyst in next generation bio-fuel cell.

1. Introduction

The preparation of high-quality 2D graphene sheets with the synergistic combination of versatile properties like high electrical/thermal conductivity[1-5] flexible but strong mechanical properties[6,7] high thermal/chemical stability[8] and extremely large surface area within 2D interface is the first and most crucial step, for successful realization of real-life applications in nanoelectronics[9,10] sensors,[11,12] nanocomposites, batteries,[12] supercapacitors and hydrogen storage, energy harvesting.

Recent interest in understanding properties of graphene has led many theoretical and experimental efforts to explore the possibility of graphene exfoliation through a combination of oxidation and sonication procedures, followed by reduction through various chemical methods[13-16] for example Stankovich et al.[13,14] and Wang et al.[16] used hydrazine-hydrate and hydroquinone as the of exfoliated GO sheets   Kamat et al. proposed photocatalytic reduction of graphite oxide with TiO_2 whereas Kundu et al. used positively charged cysteamine capped CdTe quantum dot to reduce GO under photoexposer.[17(a)-(b)]

However, the electronic properties may be interfered by these excessive reducing agents and further limit the application with precise controllability.[18] In addition, reduced graphene oxide (RGO) produced in suspension often aggregates due to van der Waals interaction. This could lead us to venture in the exploration of using photo excited CHL-a molecules as reducing as well as dispersive agent. In photosynthetic reaction centre, energy harvested through self-organised CHL-a molecules where energy is transferred via a sequence of quantum mechanical energy-transfer processes across a total distance of ~20-100 nm with near-unit quantum efficiency[19(a)] towards a reaction centre[19(b)] where electrons are donated from the photo excited CHL-a molecules to a closely packed pheophytin. The faster forward reaction[19(c)]of few picoseconds time window is ensured by geometric arrangement of closely packed pigments. Our aim is to use this photo generated electron of CHL-a to reduce GO in water which eventually give rise to tuneable functionalised graphene by controlling reduction degree. Due to its high work function (4.42 eV),[19(d)] GO can accept photo-generated electrons from the lowest unoccupied molecular orbitals (LUMOs) of CHL-a and can potentially contribute the formation of functional graphene nanosheets through reduction (Fig. 1). Khaderbad, et al used

RSC Advance

RSCPublishing

FULL PAPER

metallo-porphyrin for photo-catalytic reduction of graphene in ethanolic solvent[19(e)]. We propose to reduce graphene in aqueous solvent where after being oxidised, the photo-chemically generated CHL-a radical can have the potentiality to acquire electron through water splitting by virtue of coming back to ground state. In our previous publication we reported synthesis of RGO/CHL-a nanohybrid, through CHL-a exfoliation and showed that CHL-a can effectively tune the Fermi velocity in extended molecular frame work of graphene, eventually making it highly functional in advanced molecular electronics. The data suggested that the π-conjugated planner tetra-pyrrol structure of the CHL-a can be easily π-stacked over the surface of the sp2 hybridized RGO surface and gives rise to the RGO/CHL-a nano-hybrid[19(f)].
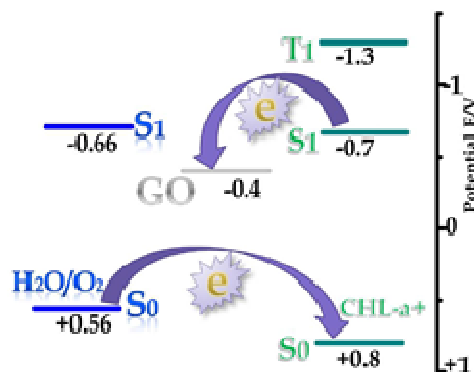
Fig: 1 Potential energy diagram showing the chemical processes possibly involved in the cathodic and anodic currents of CHL-a nanohybrid.

Therefore, it may be postulated that the transfer of the electron from the energy level of the excited CHL-a unit to the energy level of GO results in healing the defects of GO and thus reduces GO to RGO. The photo-excited CHL-a can be readily π-stacked over the RGO surface as well as get protonated. This results in formation of CHL-a$^+$ radical cation, which might favor the oxidation of water with oxygen evolution, a process that proceeds with a decrease in Gibbs enthalpy. The ground state redox potentials of the CHL-a/CHL-a$^+$ and CHL-a/CHL-a$^-$ couples are -0.94v and -0.80v (SHE) obtained from cyclic voltammetry measurements in different solvents[20]. The excited-state redox potentials of CHL-a were obtained by ascribing 1.85 and 1.33 eV to the singlet and triplet excitation energies[21].

The Water photo-oxidation with oxygen evolution catalyzed by hydrated oligomers of CHL-a immobilized at the interface between two immiscible liquids, on a bilayer lipid membrane or on an electrode has often been reported[22] Hence we also explore the possibility of using this photochemically RGO/CHL-a nanohybrid as the possible electrocatalyst through cyclic voltammetry, to be used for oxygen reduction in energy conversion systems.

2. Experimental

Preparation of Graphene Oxide (GO):

We use exfoliated GO prepared by oxidizing graphite flakes in acidic medium as the starting material for the preparation of graphene according to the modified method of Hummer's[23].

A wide range of oxygen groups bonded onto the surface of GO increases the charged concentration, thereby, increasing the dispersion of GO in water to a greater extent, with which CHL-a molecules were added with increasing concentration of 10^{-7}, 10^{-6}, 10^{-5} mole, along with 30 mints xenon lamp irradiation from a distance of 45 cm. The intensity measured was 80 mW cm^2. GO reduction proceeds with the appearance of black dispersed material from brownish yellow, suggesting the restoration of electronic conjugation. The characterization of morphological studies and the detailed structural features were investigated using high-resolution transmission electron microscopy (HRTEM; JEOL 2100). Raman spectra of the samples were recorded at room temperature in solution phase.

The light irradiation dependent study was done after different irradiation times with a white light source compiled with a <420 nm cut off filter. Room temperature optical absorption spectra were taken by a UV−vis spectrophotometer (Perkin Elmer). Room temperature photoluminescence studies were carried out using a Fluoro Max-P (Horiba Jobin Yvon) luminescence spectrometer. For time correlated single photon counting (TCSPC) measurement, the samples were excited at 375nm by picoseconds NANO-LED IBH-375. The fluorescence decays were collected on a Hamamatsu MCP photomultiplier. The following expression was used to analyze the experimental time-resolved fluorescence decays,

P(t) Here, n is the number emissive species, b is a baseline correction ("dc" offset), and α_i and τ_i are the pre-exponential factors and excited-state fluorescence lifetimes associated with the ith component, respectively. For multiexponential decays (n), the average lifetime, ⟨τ⟩, was calculated from eq 2.

$$p(t) = b + \sum_{i}^{n} \alpha_i \exp[-\frac{t}{\tau_i}] \quad (1)$$

$$\langle \tau \rangle = \frac{\sum_{i=1}^{n} a_i \tau_i^2}{\sum_{i=1}^{n} a_i \tau_i} \quad (2)$$

3. Results and discussion

TEM analysis:

The formation of GO has been confirmed through TEM showing crystalline lattice surrounded by amorphous zone [Fig. 2 A (a), (b)] and formation of RGO after steady state photo

RSC Advances Accepted Manuscript

RSC Advance

RSC**Publishing**

exposure of CHL-a/GO homogenous aqueous mixture which clearly shows evolution of crystalline graphene lattice at highest CHL-a concentration [Fig. 2 B (a), (b)] in comparison with bare GO counterpart. The interactive affinity between CHL-aand RGO is ensured through π-π interaction and can render the platform for GO to be reduced via CHL-a molecules in closely packed environment. The SAED pattern with final CHL-a concentration clearly shows bright hexagonal inner circle, which gradually faded towards outer region. Although few bright spots in outer region, signifying the folded RGO or stacked macrocycle of CHL-a over RGO surface, are clearly visible.[24]
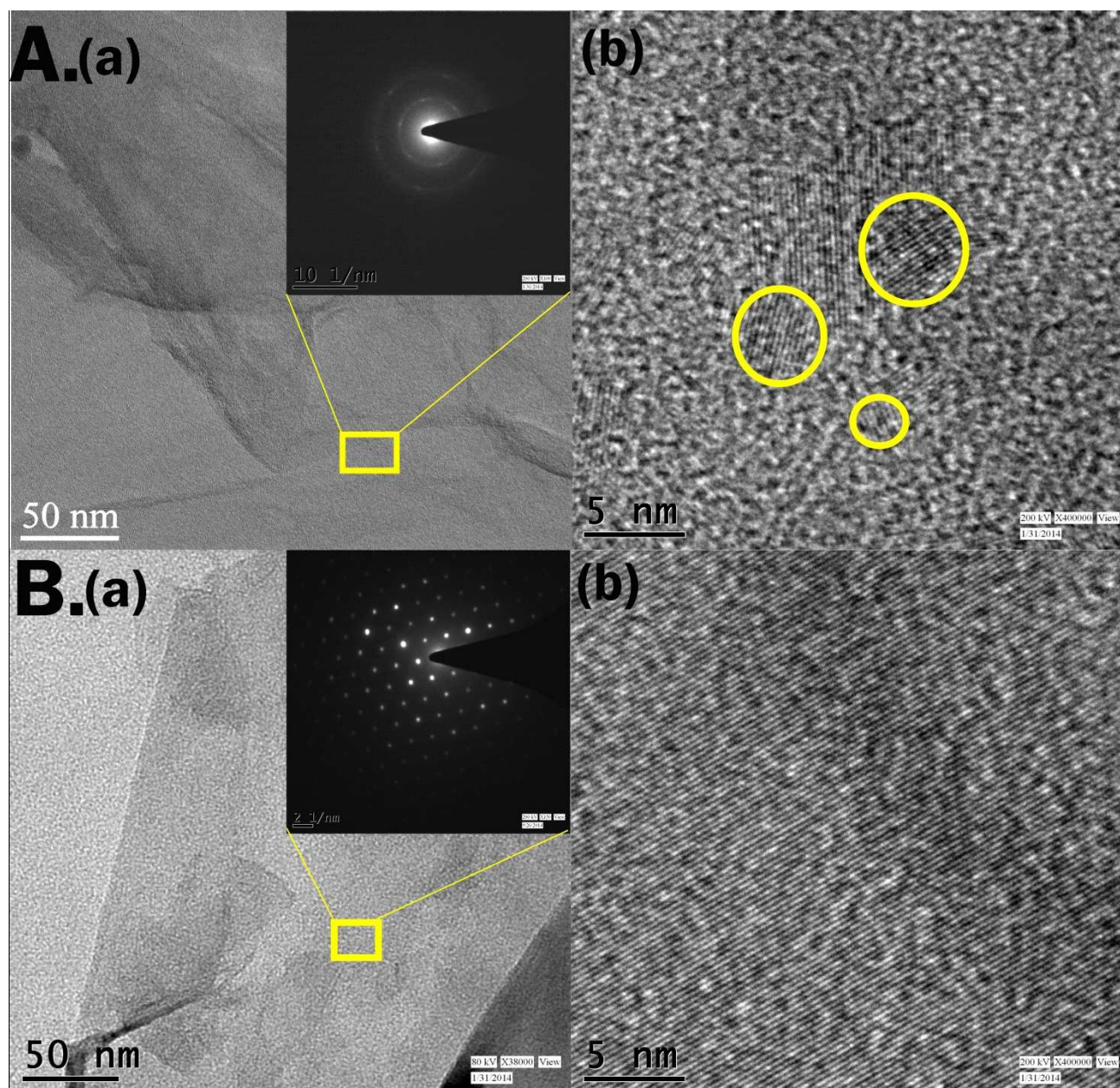
Fig. 2 TEM & SAED image of [A. (a), (b)] GO yellow circles are showing the crystalline zones with in the amorphous domain & [B. (a), (b)] RGO/CHL-a highest concentration.

RSC Advance

RSC**Publishing**

FULL PAPER

XRD analysis:

The sharp (002) diffraction peak at 2Ө=10.8° and the broad diffraction peak 2Ө = 22.8° appeared at the XRD spectra of GO and the RGO/CHL-a respectively Fig. 3 signifies the evidence of GO reduction in presence of CHL-a, corroborates with evidences in the literature[24(b)]. The appearance of broad peak in nanohybrid indicates that the sheets of nanohybrids are poorly ordered[24(e)]. In addition, the effective CHL-a functionalization in graphene was verified by the disappearance of the proper intense diffraction peak in the XRD pattern. This clearly demonstrates the creation of a fully π stacked CHL-a/RGO sheets.
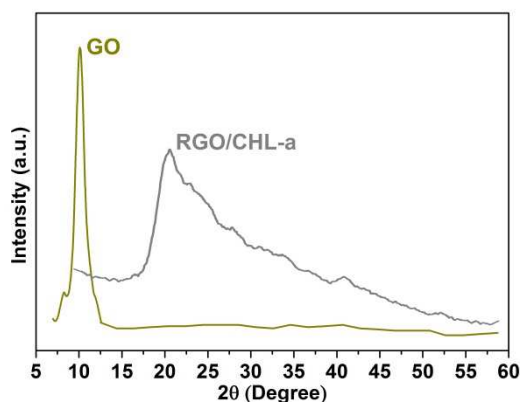
Fig. 3 XRD spectra of GO & RGO/CHL-a nano-hybrid with 10^{-5} mole of CHL-a concentration.

XPS analysis:

The high-resolution Carbon 1s XPS spectrum of the GO sheets shows a sharp peak at around 284.6 eV that corresponded to C-C bonds of carbon atoms in a conjugated honey-comb lattice. Peaks at 286.7, 288.4 and 290.1 eV can be attributed to different sp3 bonding configurations due to the harsh oxidation and destruction of the sp2 atomic structure (Fig. 4 (A)) [24(f)]. After reduction with CHL-a, the intensities of all of the related oxygen peaks except C=0 were profoundly decreased in the RGO/CHL-a sample [conc. of 10^{-5} mole] compared to GO, indicating that the delocalized π conjugation was restored in our RGO/CHL-a sample (Fig. 4 (B). The intensity of C=0 peak increased due to the contribution of CHL-a carbonyl group. Based on the XPS analyses, the as-prepared GO had a very low delocalized π conjugation percentage 14.58%. In contrast, the RGO/CHL-a produced by CHL-a reduction was 57.2% (Table1). We concluded that the RGO from our process contained far less oxygen, confirming its high quality. The main peak, of the high-resolution Nitrogen 1s XPS spectrum N-1, at a binding energy of 398.1–398.9 eV in CHL-a (Fig. 4 (C)) is characteristic of the pyrrolenine nitrogen atoms of the

porphyrin macrocycle of CHL-a. A second peak (N-2), a shoulder, in the XPS of CHL-a alone can also be seen at 400 eV. It is most likely due to the protonated nitrogen, produced as a result of a small degree of demetallation of CHL-a during its exposure to X-rays in the course of the experiment[24(g)]. In RGO/CHL-a hybrid we found the most intense peak N-3 at around 408.4ev, indicating most of the nitrogens of CHL-a remains in the oxidised form or positively charged over graphene surface, where the expulsion of the core electrons from CHL-a -nitrogen has become more difficult, thereby needing a comparatively higher energy, i.e., 408.4 eV. The positively charged nitrogen evolved due to the transfer of non-bonding electrons on nitrogens of CHL-a, to GO after photoexposure as a consequence reduced RGO is being formed.

RSC Advance

RSC**Publishing**

FULL PAPER

(A)

Legend: GO, sp² C, C-O, C=O, O-C=O

(B)

Legend: RGO/CHL-a, sp² C, C-O, C=O, O-C=O

(C)

Legend: RGO/CHL-a, CHL-a, N3, N2, N1
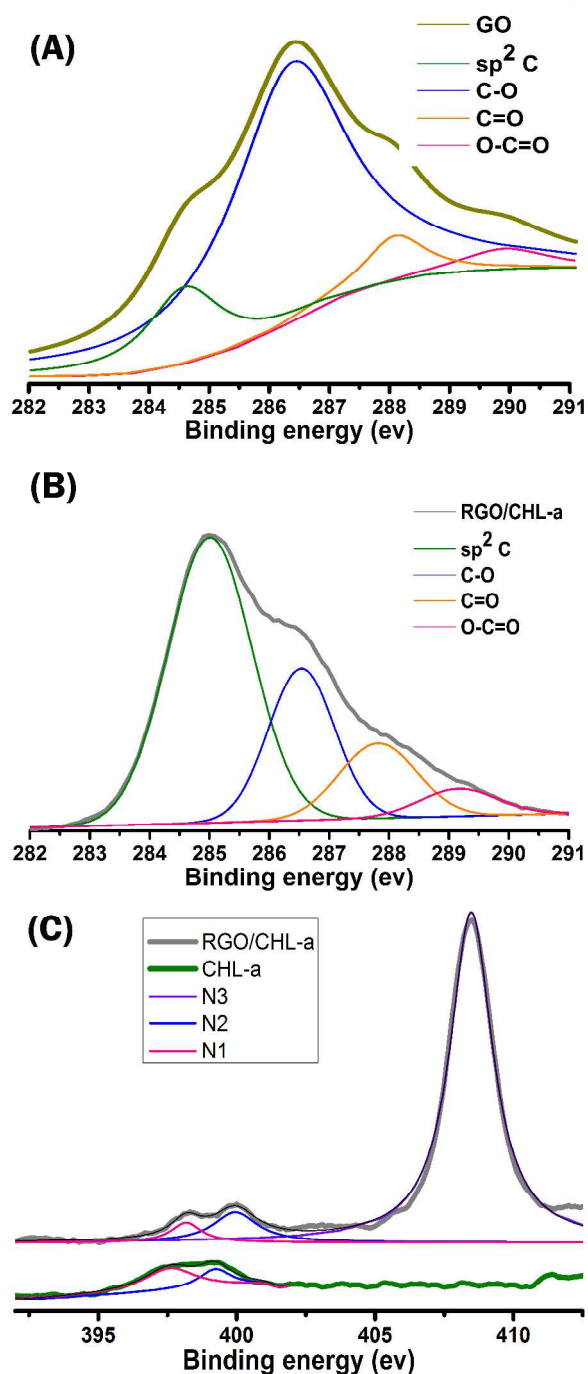
Fig. 4. (A) & (B) Carbon 1s XPS spectra of GO & RGO/CHL-a nano-hybrid with 10^{-5} mole of CHL-a concentration respectively. (c) Nitrogen 1s XPS spectra of RGO/CHL-a & CHL-a nano-hybrid (10^{-5} mole) of CHL-a concentration.

Table1. High resolution XPS data of C 1S peak area contributions of all Samples:

Sample	sp^2C at 284.6 eV (%)	C-O at 286.7 eV (%)	C=O at 288.4 eV(%)	O–C=O at 290.1eV (%)
GO	14.58	72.54	7.81	5.07
RGO/CHL-a	57.30	23.88	13.77	5.05

RGO/CHL-a = 10^{-5} mole of CHL-a concentration.

Uv-vis Absorption spectroscopy:

The signature of GO reduction can also be observed through the Uv-vis absorption spectroscopy. The gradual increment of 270 nm absorbance peak-intensity at the expense of 230 nm GO peak with increasing CHL-a concentration, proves the restoration of sp² network in GO [Fig. 5 A.]. The ratio of 230 nm to 270nm intensities decreases from 1.41 to 1.02 for GO to highest concentration CHL-a reduced GO, [Fig. 5 A. inset]. This phenomenon implies that the contribution of 270nm absorbance is more pronounced than the 230nm absorbance due to enhancement of GO reduction with increasing CHL-a concentration. An apparent colour change of the GO solution from light yellow to black was observed due to the progressive formation of RGO under photo-excited CHL-a reduction with increasing concentration [Fig. 5 A. inset]. The Uv-vis absorption spectra of varying conc. of CHL-a without GO is given in supporting information.

Photoluminescence spectroscopy & TCSPC:

This can be further supported by the gradual quenching of Photoluminescence spectra at 675nm with increasing CHL-a concentration in GO after photo exposure. The presence of CHL-a enhances the sp² restoration process of GO under photo excitation which further corroborates the probability of π stacking and leads to electron transfer from CHL-a to RGO Fig. 5 (B).

The electron transfer phenomena can be understood through the TCSPC measurement. The τ values of bi exponentially fitted decay curves are given in Table 2 indicate the presence of increased conformational heterogeneity[25]. The profound decreases in fluorescence average lifetime <τ> with increasing CHL-a concentration may be correlated with macrocycle distortion Fig. 5 (C) in conjunction with both internal conversion and intersystem crossing to the CHL-a porphyrin ring[26].

This phenomena leads us to interpret the increased rates of internal conversion of π-π* to the ground state, arising from an enhanced Franck-Condon factor associated with structural reorganization in the excited state. Whereas the enhanced intersystem crossing from π-π* was attributed to increased spin-

RSC Advance

FULL PAPER

orbit coupling caused by the non-planarity of the CHL-a macrocycle. As a consequence significantly lower fluorescence yields, large Stokes shifts, and shorter lifetimes of the lowest excited state are expected to be evident due to the combined effects of destabilization and stabilization of energy levels, which ultimately result in a further reduction of the energy gap between HOMO and LUMO[27].

In our system no stock shift is evident, instead the intensity of CHL-a emission gradually reduces with increasing CHL-a concentration [Fig. 5. (B).]. When GO is not added with CHL-a with same concentration the life time is very close to monomeric CHL-a life time (4.42 ns). Thus it can be inferred that intersystem crossing and internal conversion is negligible in our system. In summary, excluding the above mentioned possibility of internal conversion and intersystem crossing, we can attribute the decrease in luminescence intensity to the fact that with increasing CHL-a concentration while other parameters like distance and exposure time are constant more amount of CHL-a participates in restoration of sp2 network of GO through photo-generated electron donation from CHL-a to GO. The GO/CHL-a interaction is mostly ensured through π stacking of CHL-a macrocycle over almost planar GO surface. The two lifetimes, observed for CHL-a with electron-withdrawing GO can be described as resulting from two conformations. We attribute the shorter lifetime component to the conformation in which electron transfer is efficient and the longer component to the conformation in which electron transfer is relatively inefficient. Since the later one is very close

to monomeric CHL-a, we can assume that this longer lifetime component signifies the geometry of monomeric porphyrin molecules which remain unreacted with GO within solution.

Raman spectroscopy:

Raman spectra gives clear insight in support of the formation of RGO where photo-excited electron can be donated from CHL-a to GO. The G band and D band is usually assigned to the E_{2g} phonon of C sp2 atoms and breathing mode of k-point phonons of A_{1g} symmetry respectively for the graphene[28(a)]. The appearance of a prominent D band in the spectrum is also an indication of disorder in graphene owing to presence of oxide functional groups[28(b)]. It has been well observed that the size of the defect-free sp^2 cluster regions is the inverse of the ratio of D and the G band integrated intensities (I_D/I_G)[28(c)].

Here, the ratio of I_D/I_G exhibits a significant decrease with the increasing CHL-a concentration in comparison to the previously reported RGO formation process after chemical reduction where the increased I_D/I_G ratio has been reported[29].

In presence of increasing concentration of [10^{-7}, 10^{-6}, 10^{-5} mole] CHL-a molecules, the corresponding I_D/I_G ratio of the as-prepared RGO is 1.1, 1.07, 1.05 and 1.01, respectively (Fig. 5. (D)). We conclude that the production of RGO from GO by reduction with CHL-a can have a healing effect[30], the photo excited CHL-a molecules can further recover the aromatic structures by repairing defects of GO by donating electron from the excited state.

RSC Advance

RSC**Publishing**
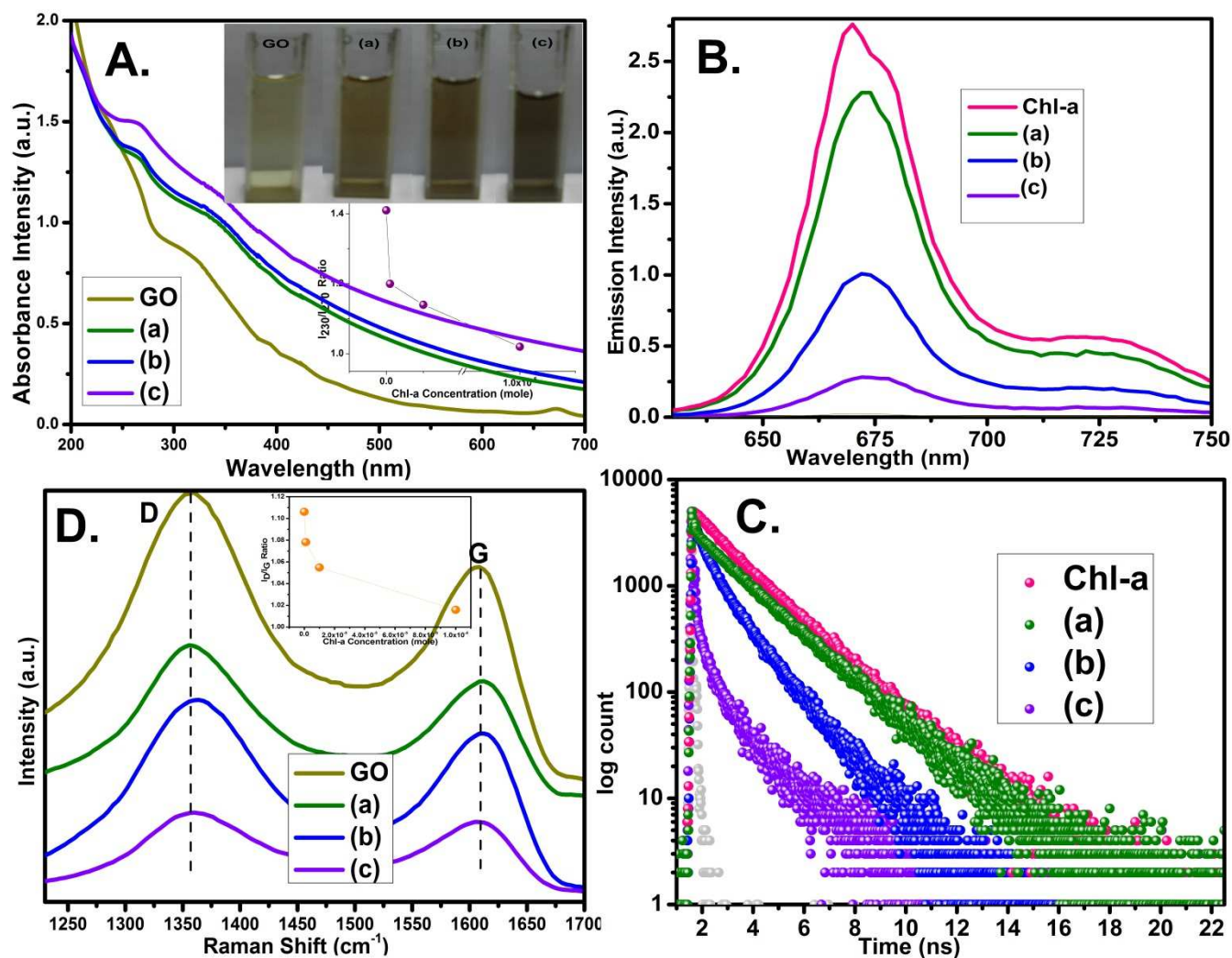
Fig. 5 A. Uv-vis absorption spectra (inset showing colour of the samples & ratios of 230nm to 270nm intensities), B. photoluminescence spectra, C. TCSPC data and D. Raman spectra (inset showing I_D/I_G ratios of intensities)of nanohybrid with 10^{-7}, 10^{-6}, 10^{-5} mole of CHL-a concentration from (a) to (c) respectively.

Table2. Decay Time Components of All Samples (Excitation at 405 nm; Emission at 673nm)

Sample	τ_1 (ps)	a_1	τ_2(ns)	a_2	$<\tau>$(ns)	$\chi2$	Quantum yield (±3%)	Rad.rate (k_{rad}) (ns^{-1}) (±6%)	Non-Rad.rate (k_{nrad}) (ns^{-1}) (±6%)	k_{rad}/k_{nrad}
(a)	640.16	31.07	4.24	68.93	4.01	1.13	0.24	0.059	0.189	0.312
(b)	611.72	58.73	3.81	42.27	3.22	1.11	0.17	0.052	0.257	0.202
(c)	506.86	78.09	2.07	21.91	1.26	1.23	0.15	0.119	0.674	0.172
CHL-a	889.07	11.30	4.68	88.70	4.59	1.15	0.30[a]	6.535	0.152	-----

(a),(b),(c)=RGO/CHL-a nanohybrids with 10^{-7}, 10^{-6}, 10^{-5} mole of CHL-a concentration respectively. $\chi2$=Curve fitting residual parameter. [a]Taken from ref.[32], k_{rad} =RGO/CHL-a radiative decay rate, k_{rad} = monomeric CHL-a radiative decay rate.

RSC Advance

FULL PAPER

Cyclic voltammetry measurement:

By virtue of having further insight about the reduction of GO through adsorbed or π-stacked CHL-a molecules we peep into the world of electrochemical measurement where glassy carbon [GC] electrode has been coated with RGO with increasing CHL-a concentration by drop casting, and the electrolyte pH was maintained around 7 (neutral) against Ag/AgCl electrode.

The cyclic voltammetry in Fig. 6, shows the photo excited CHL-a molecules mediate electron transfer from the electrode to oxygen functional group on the GO sheet. The hole, on the other hand, is expected to be transferred to water which acts as hole acceptor and is oxidized. The water reduction potential is around 0.5v more positive than chl/chl+ pair[31]. Thus the resulting Chl+ radical cation may oxidize water with oxygen evolution, a process that proceeds with a decrease in Gibbs enthalpy, as shown by the energy diagram of Fig. 1. Interestingly very distinguished characteristics are observed both in positive and negative shift of the potential. The GO cathodic peak at -0.62v and anodic peak at 0.46v reduces with CHL-a concentration with the gradual evolution of cathodic peak at -1.7v and 0.4v. We propose the reason based upon the probability that CHL-a on RGO surface is restored back in neutral form accepting the electron from aqueous environment after photo exposure. In positive electrode potential the electrostatic interaction between positively charged GC electrode and the electron cloud of RGO renders the macromolecules to get into a different orientation through the less involvement of π-electron into π-stacking of CHL-a and RGO. Thus the C=O of CHL-a cannot participate in the reduction process. The C=O reduction peak cannot be observed, Hence 0.46v anodic peak which disappears in second cycle [Fig: 6 (B)] may be attributed towards the C=O impurities present as defect in GO. The 1st cycle cathodic peak at 0.4v may be attributed to the reduction peak of CHL-a, carbonyl group. This group is likely to be oriented closer to the electrode in reverse sweep and accepts electron to get reduced,[31] thus rendering the reduction reaction possible. This C=O peak retains in second cycle only for the CHL-a/RGO hybrids, signifying that the formation oof RGO[after photo exposure] renders the planar CH-a molecules to π-stack over graphene surface more firmly and allows the electron to take part in the subsequent carbonyl reduction. Thus we could not find any peak in bare GO and GO with CHL-a without photo exposure. If CHL-a molecules would have desorbed from RGO surface in positive run we could not have found the 0.46v anodic peak. Thus we attribute the appearance of 0.46v anodic peak towards the reduction of carbonyl group of CHL-a. The intensity of this peak decreases with the increasing CHL-a concentration as the gradual appearance of RGO. Interestingly when we compare the GO with that of CHL-a reduced counterpart, the major difference found in the appearance of -1.7v cathodic peak. This peak also found in CHL-a reduced RGO where the intensity increases towards higher CHL-a concentration. The potential of the $Chl+/Chl^{2-}$ couple is -1.57v, estimated from the cyclic voltammogram of a CHL-a solution in DMF[31]. Thus it is highly unlikely to assign this peak towards the oxidation of macrocycle in such a higher negative potential. The disappearance of porphyrin redox wave may be attributed to the staking of the porphyrin macrocycles, which prevents the reduction of the ring at the cathode. The CHL-a assembly behave differently in terms of its redox property than that of monomeric one as it is π-stacked over graphene surface. Thus we assign this -1.7v peak to the oxygen reduction in neutral ph in aqueous NaCl electrolyte which retains in second cycle proving reversibility. The cyclic voltammetry of CHL-a without GO is given in supporting information.

The oxygen reduction reaction (ORR) in aqueous solutions occurs mainly by two pathways: the direct 4-electron reduction pathway from O_2 to H_2O, and the 2-electron reduction pathway from O_2 to hydrogen peroxide (H_2O_2). In proton exchange membrane (PEM) fuel cells, including direct methanol fuel cells (DMFCs), ORR is the reaction occurring at the cathode. In our experiment the overall reaction mechanism can be as follows: In the first step, the adduct between oxygen and the Mg center of the macrocyclic compound is formed, followed by an intra-adduct electron transfer from the Mg ion to the oxygen. Alt et al. explained[32] that in the interaction between O_2 and magnesium Mg centre electron transition occurs first from oxygen into the empty d_{z2} orbital, forming a σ bond, lowering the anti-bonding π orbitals and raising the energy of the d_{xz} and d_{yz} orbitals of the center magnesium, thus allowing the electron transition from these filled orbitals to the anti-bonding π orbital, and resulting in enhanced interaction. The addition of protons from the electrolyte, together with the electron transfer, then produces H_2O_2 at 0.7 volt. The H_2O_2 is not the final product and can be further reduced to produce water at potential 1.7 volt, resulting total 4 electron reduction of oxygen in CHL-a graphene surface. The mechanism can be summarized as follows:

$$[LMg^{II}] + O_2 \leftrightarrow [LMg^{\delta+}\ldots\ldots\ldots O_2^{\delta-}]$$
$$[LMg^{\delta+}\ldots\ldots\ldots O_2^{\delta-}] + H^+ \rightarrow [LMg^{III}\ldots\ldots\ldots O_2H]^+$$
$$[LMg^{III}\ldots\ldots\ldots O_2H]^+ + H^+ + 2e^- \rightarrow [LMg^{II}] + H_2O_2$$
$$H_2O_2 + 2H^+ + 2e^- \rightarrow 2H_2O$$
$$H_2O_2 \rightarrow H_2O + \tfrac{1}{2} O_2$$
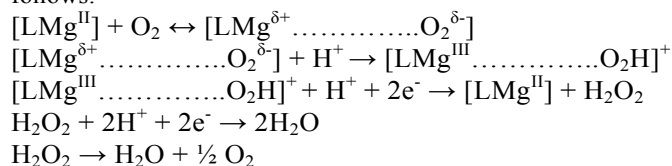
Where L represents the ligand and Mg is the magnesium centre. The -0.7v cathodic wave at the second cycle [Fig: 5 (B)] decreases for the first two concentration due to the formation of

RSC Advance

RSCPublishing

FULL PAPER

RGO and reappear in highest CHL-a concentration accompanied by a concomitant increase in the peak current density, as the first reduction wave of above mentioned equation the trend remain same in following cycle.

All these data cumulatively suggests the presence of CHL-a over graphene surface and indicates the photoexcited CHL-a in aqueous environment can restore back to its neutral stage acquiring electron from surrounding water. Thus there is always a possibility of water splitting in due course. Although further study in this regard is necessary to prove water splitting, we can surely say that this one-pot process of preparing RGO/CHL-a nanohybrid paved the way to architect next generation electrode material where CHL-a over graphene surface can effectively contribute the oxygen reduction mechanism on cathode and under pins clean-energy technology such as bio-fuel cells and metal–air-batteries.

Fig: 6 (A) Cyclic voltammetry profiles of electrochemical reduction and oxydation of nanohybrid with increasing CHL-a concentration 10^{-7}, 10^{-6}, 10^{-5} mole in (a), (b) & (c) respectively in first cycle. (B) Cyclic voltammetry profiles of electrochemical reduction and oxydation of nanohybrid with increasing CHL-a concentration 10^{-7}, 10^{-6}, 10^{-5} mole in (a), (b) & (c) respectively in second cycle. Conditions: NaCl 50 mM, pH 7.2 background electrolyte. Scan rate: 100 mV s^{-1}.

4. Conclusions

We tried to unravel the process of restoration of sp2 hybridization in GO framework where photo excited electron can be transferred from CHL-a LUMO to GO. This can be ensured via π interactive affair between CHL-a and RGO surface. The formation of crystalline RGO lattice [evident from TEM data] along with the gradual reduction of I_D/I_G ratio in Raman spectra points towards the evolution of RGO with increasing CHL-a concentration. This phenomenon further corroborates with the TCSPC data where the contribution of faster decay component increases with CHL-a concentration signifies the electron transferprocess from chla to graphene oxide and supported by C1s xps spectra showing increased intensity of sp3 binding energy at the expense of c=0 binding energy at….. The presence of intense N1s spectra at higher energy 408 ev also supports the electron transfer from chla non bonding electron to graphene surface. The ratio of radiative to non-radiative decay rate decreases along with the CHL-a concentration also implies efficient electron transfer from CHL-a to GO. Interestingly when we compare the data of GO with that of CHL-a reduced counterpart, through cyclic voltammetry in aqueous NaCl environment. The major difference found in the appearance of -1.7v cathodic wave. This peak also found CHL-a reduced RGO where the intensity increases towards higher CHL-a concentration and can be attributed towards 4 electron oxygen reduction pathway. The 0.7v anodic wave super imposes with the GO peak, thus we cannot differentiate it for the first two concentrations, from the first step of O_2 reduction leading to H_2O_2 production. Interestingly at final CHL-a concentration this peak is much intense along with the -1.7 v peak in contradiction to other data, and shows highest possible reduction of GO. Thus it can be ascribed to the first reaction of oxygen reduction. The overall probable mechanism has been proposed. All these findings in combination bring a deeper understanding of RGO production in simple bio friendly route, by accepting electron from photo excited CHL-a and simultaneously propose that this RGO CHL-a nanohybrid can be used as an effective electron transfer catalyst in next generation bio-fuel cell.

RSC Advances Accepted Manuscript

RSC Advance

RSC**Publishing**

FULL PAPER

Notes and references

[a] Metallurgy & Material Engineering Department, Jadavpur University, Kolkata 700032, India.
[b] School of Materials Science & Nanotechnology, Jadavpur University, Kolkata 700032, India.
c Henry W Bloch School of Management,UMKC,Kansas,Missourie,USA
E-mail: jhimlisarkar0@gmail.com; Tel: +91 9831566632

† The manuscript was written through contributions of all authors. All authors have given approval to the final version of the manuscript. † These authors contributed equally.

Electronic Supplementary Information (ESI) available: [details of any supplementary information available should be included here]. See DOI: 10.1039/b000000x/

References

1. K. S. Novoselov, A. K. Geim, S. V. Morozov, D. Jiang, Y. Zhang, S. V. Dubonos, I. V. Grigorieva, A. A. Firsov, *Science*, 2004, **306**, 666–669.
2. A. Balandin, S. Ghosh, W. Bao, I. Calizo, D. Teweldebrhan, F. Miao, C. N. Lau, *Nano Lett.,* 2008, **8,** 902–907.
3. G. Eda, G. Fanchini, M. Chhowalla, *Nat. Nanotechnol.* 2008, **3,** 270–274.
4. K. S. Kim, Y. Zhao, H. Jang, S. Y. Lee, J. M. Kim, K. S. Kim, J-.H. Ahn, P. Kim, J-.Y. Choi, B. H. Hong, et al. *Nature*, 2009, **457**, 706–710.
5. S. Park, R. S. Ruoff, *Nat. Nanotechnol.* 2009, **4**, 217–224.
6. X. Li, X. Wang, L. Zhang, S. Lee, H. Dai, *Science*, 2008, **319,** 1229–1232.
7. V. C. Tung, M. J. Allen, Y. Yang, R. B. Kaner, *Nat. Nanotechnol.* 2009, **4**, 25–29.
8. H. K. Chae, D. Y. Siberío-Pérez, J. Kim, Y. Go, M. Eddaaoudi, A. J. Matzger, M. O'Keeffe, O. M. Yaghi, *Nature* 2004, **427**, 523–527.
9. P. Avouris, Z. Chen, V. Perebeinos, *Nat. Nanotechnol.* 2007, **2,** 605–615.
10. Y. W. Son, M. L. Cohen, S. G. Louie, *Nature* 2006, **444,** 347–349.
11. F. Schedin, A. K. Geim, S. V. Morozov, E. M. Hill, P. Blake, M. I. Katsnelson, K. S. Novoselov *Nat. Mater.* 2007, **6,** 652–655.
12. S. Pour, M. T. Ahmadian, A. Vafai, *Solid State Commun.* 2008, **147,** 36–340.
13. S. Stankovich, R. D. Piner, X. Q. Chen, N. Q. Wu, S. T. Nguyen, R. S. Ruoff, *J. Mater. Chem.* 2006, **16**, 155–158.
14. S. Stankovich, D. A. Dikin, R. D. Piner, K. A. Kohlhaas, A. Kleinhammes, Y. Y. Jia, Y. Wu, S. T. Nguyen, R. S. Ruoff, *Carbon* 2007, **45**, 1558–1565.
15. D. Li, M. B. Muller, S. Gilje, R. B. Kaner, G. G. Wallace, *Nat. Nanotechnol.* 2008, **3**, 101–105.
16. G. X. Wang, J. Yang, J. Park, X. L. Gou, B. Wang, H. Liu, J. Yao, *J. Phys. Chem. C* 2008, **112**, 8192–8195.
17. (a) G. Williams, B. Seger, P. V. Kamat, *ACS Nano* 2008, **2**, 1487–1491.
    (b) S. Kundu, S. Sadhu, R. Bera, B. Paramanik, and A. Patra *J. Phys. Chem. C* 2013, **117**, 23987−23995
18. Y. Hernandez, V. Nicolosi, M. Lotya, F. M. Blighe, Z. Y. Sun, S. De, I. T. McGovern, B. Holland, M. Byrne, Y. Gunko, et al. *Nat. Nanotechnol.* 2008, **3**, 563–568.
19. (a) G. D. Scholes, *J. Phys. Chem. Lett.* 2010, **1**, 2−8.
    (b) G. D. Scholes, G. R. Fleming, A. O. Castro, R. van Grondelle, *Nat. Chem.* 2011, **3**, 763-774
    (c) D. I. G. Bennett, K. Amarnath, G. R. Fleming, *J. Am. Chem. Soc.* 2013, **135**, 9164−9173
    (d) G. Giovannetti, P. A. Khomyakov, G. Brocks, V. M. Karpan, J. van den Brink, P. J. Kelly. *Phys. Rev. Lett.* 2008, **101**, 026803.
    (e) M. A. Khaderbad, V. Tjoa, T. Z. Oo, J. Wei, M. Sheri, R. Mangalampalli, V. R. Rao, S. G. Mhaisalkarb, N. Mathews, *RSC Adv*., 2012, **2**, 4120-4124.
    (f) D. Das , J. Sarkar Manna, M. K. Mitra, *J. Ph. Chem. C* 2015, **119**, 6939−6946.
20. T. Watanabe, M. Kobayashi, in: H. Scheer (Ed.), The Chlorophylls, CRC Press Inc, Boca Raton, FL, 1991, p. 287.
21. G. R. Seely, *Photochem. Photobiol*. 1978, **27**, 639.
22. G. Volkov, M.I. Gugeshashvili, D.W. Deamer, *Electrochim. Acta* 1995, **40**, 2849.
23. Z. T. Luo, Y. Lu, L. A. Somers, A. T. C. Johnson, *J. Am. Chem. Soc.* 2009, **131**, 898.
24. (a) J. H. Warner, Y. Fan, A. W. Robertson, K. He, E. Yoon, G. D. Lee, *Nano Lett.* 2013, **13**, 4937−4944.

RSC Advances Accepted Manuscript

RSC Advance

FULL PAPER

(b) J. Shen, Y. Hu, M. Shi, X. Lu, C. Qin, C. Li, M. Ye, *Chem. Mater.* 2009, **21**, 3514.

(c) N. A. Kumar, H. J. Choi, Y. R. Shin, D. Chang, L. Dai, J. B. Baek, *ACS Nano,* 2012, **6**, 1715.

(d) C. Fu, G. Zhao, H. Zhang and S. Li, Int. *J. Electrochem. Sci.*, 2013, **8**, 6269.

(e) M. Zainy , N. M. Huang , S. V. Kumar , H. N. Lim , C. H. Chia , I. Harrison , *Mater. Lett.* 2009, **89**, 180.

(f) J. Kauppila, L. Lund, T. Laiho, M. Salomaki, J. Kankare, J. Lukkaria, *J. Mater. Chem. C*, 2014, **2**, 3602–3609.

(g) S. Barazzouk, L. Bekale, S. Hotchandani, *J. Mater. Chem.*, 2012, **22**, 25316.

25. N. Aratani, D. Kim, A. Osuka, *Accounts of Chemical Research.* 2009, **42**, 1922-1934.

26. S. Gentermann, C. J. Medforth, T. P. Forsyth, D. J. Nurco, K. M.Smith, J. Fajer and D. Holten, *J. Am. Chem. SOC.*, 1994, **116**, 7663.

27. N, C. Maiti, M. Ravikanth, *J. Chem. Soc., Faraday Trans.,* 1996, **92**, 1095-1100.

28. (a) A. G. Nandgaonkar, Q. Wang, K. Fu, W. E. Krause, Q. Wei, R. Gorga, L. A. Lucia, *Green Chem*., 2014, **16**, 3195.

(b) C. K. Chua, A. Ambrosi, M. Pumera *J. Mater. Chem*., 2012, **22**, 11054

(c) L. G. Cancado, K. Takai, T. Enoki, M. Endo, Y. A. Kim, H. Mizusaki, A. Jorio, L. N. Coelho, R. Magalhaes-Paniago, M. A. Pimenta, *Appl. Phys. Lett*. 2006, **88**. 163106.

29. S. Stankovich, D. A. Dikin, R. D. Piner, K. A. Kohlhaas, A. Kleinhammes, Y. Jia, Y. Wu, S. T. Nguyen, R. S. Ruoff, *Carbon* 2007, **45**, 1558–1565.

30. M. Zhang1, R. R. Parajuli1, D. Mastrogiovanni, B. Dai, P. Lo, W. Cheung, R. Brukh, P. L. Chiu, T. Zhou, Z. Liu, E. Garfunkel. H. He, *Small* 2010, **6**, 1100–1107.

31. F. T. Buoninsegni, L. Becucci, M. R. Moncelli, R. Guidelli, A Agostiano, P. Cosma, *J. Electroanal. Chem.* 2003, **550**, 229-240.

32. J. Sarkar Manna, D. Das, M. K. Mitra, *J. Phys. Chem. C* 2014, **118**, 6558−6564.
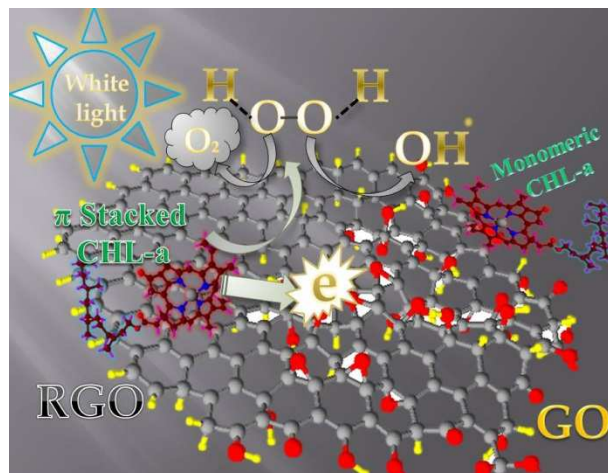
RSC Advance

RSC**Publishing**

FULL PAPER

Restoration of sp2 hybridization in GO framework where photo excited electron can be transferred from CHL-a to GO and can be ensured via π interactive affair between CHL-a and RGO surface, resulting in a formation of RGO\CHL-a nano hybrid, where CHL-a cation stabilised itself by accepting electron from aqueous environment and eventually give rise to an efficient electron transfer nano hybrid catalyst in next generation bio-fuel cell.